International Journal of Analysis and Applications

Numerical Investigation of Radiative Flow of Cu-Al_2O_3/H_2O Hybrid Nanofluid over a Moving Flat Plate

Khuram Rafique[1], Gamal Elkahlout[2,*], Samra Sajjad[3]

[1]*Centre of Excellence for Social Innovation and Sustainability, Institute of Engineering Mathematics, Universiti Malaysia Perlis, Arau, Perlis, Malaysia*

[2]*Faculty of Business Studies, Arab Open University, Riyadh, Saudi Arabia*

[3]*Department of Mathematics, University of Sialkot, Sialkot 51040, Pakistan*

**Corresponding author:* g.elkahlout@arabou.edu.sa

ABSTRACT. Researchers have shown interest in how hybrid nanoparticles can improve heat transfer, promoting further investigation into the regular fluid. This study examines the flow of hybrid nanoliquid flow with heat transfer on a moving plate, with a focus on Joule heating. Additionally, the aligned magnetic effect is incorporated for the analysis of Copper and Aluminum oxide nanoparticles combined with water as a base fluid. The PDE's complexity was reduced via a similarity transformation into an ODE system that was numerically solved for different values of governing parameters using the Keller box method. There is a unique solution available against $\lambda > 0$, while two solutions are available for $\lambda_c < \lambda \leq 0$. Additionally, it was observed that the magnetic factor enhances the energy transmission performance and increases the critical value, while no impact of the Eckert number. The outcomes of this problem are novel and innovative, with numerous practical applications in industry and engineering.

1. Introduction

A nanofluid is a fluid created by mixing nanoparticles, which typically range in diameter between 1 and 100 nanometers, in a base fluid such as oil, water, or ethylene glycol. These nanoparticles can be metallic, ceramic, or carbon-based, chosen based on their desired properties and specific applications. Common nanoparticles in nanofluids include materials such as aluminium, copper, alumina, graphite, and carbon nanotubes. Similarly, typical base

Received Jul. 13, 2025

2020 Mathematics Subject Classification. 76D05.

Key words and phrases. hybrid nanofluid; MHD; joule heating; stretching/shrinking surface; heat transfer; radiative flow; Keller box method.

https://doi.org/10.28924/2291-8639-23-2025-216

ISSN: 2291-8639

fluids are water, propylene glycol, and various oils. The field was introduced by Choi [1], who proposed the concept of nanofluids.

Recent decades have seen increased exploration of nanoparticles and nanofluids, which have advanced numerous fields due to their unique properties. Additionally, nanofluids, comprising fluids with suspended nanoparticles, have demonstrated improved thermal and mechanical characteristics, opening new possibilities for heat transfer and lubrication technologies. Parkash et al. [2] provided an analytical discussion on nanofluid flow through a channel. Huminic [3] examined nanofluid flow in mini channels, micro channels, and cavities under various physical conditions and boundary scenarios. Molana et al. [4] offered an alternative perspective on the mathematical modelling of the effective thermal conductivity of nanofluids.

Research has shown growing interest in the flow and heat transfer mechanisms of hybrid nanofluids within enclosed structures, given their wide range of applications in science and technology. Hybrid nanofluids are a recent development that builds on the concept of nanofluids composed of different nanoparticles dispersed in a base fluid. This mixture aims to enhance thermophysical and rheological properties while improving heat transfer. Aly and Pop [5] studied the heat transfer and MHD boundary layer flow of a hybrid nanoliquid flowing over a contracting or expanding sheet, considering partial slip and Joule heating. Their study demonstrated that the hybrid nanofluid is more effective than single-component nanofluids in terms of overall performance. Aladdin et al. [6] discussed the flow of a hybrid nanofluid over a permeable moving surface.

Magnetohydrodynamics (MHD) studies the behaviour of electrically conducting fluids like electrolytes, liquid metals, and plasmas under magnetic fields. In MHD, the interplay between fluid movement and magnetic forces leads to unique phenomena such as magnetic field induction, electric current generation, and changes in flow patterns. MHD applications in various fields, such as astrophysics, plasma physics, and engineering, are used to understand phenomena like solar flares, the dynamics of the Earth's magnetosphere, and the design of advanced propulsion systems and energy generation technologies. Many industry and engineering sectors heavily rely on MHD processes, including power generation, industrial operations, crystal growth, metal casting, and cooling in nuclear reactors, as noted by Zainal [7]. Goud et al. [8] studied the various impacts of stretching a porous plate, accounting for viscous dissipation. Meanwhile, Chamkha et al. [9] explored the effects of Joule heating and thermal radiation.

MHD boundary layer flow refers to the study of fluid movement close to a solid surface, where a magnetic field influences the boundary layer characteristics. This includes phenomena such as the modification of velocity profiles, heat transfer rates, and boundary layer thickness

caused by the interaction among the fluid flow, magnetic field, and solid surface. Reza-E-Rabbi et al. [10] created a model for time-dominated boundary layer flow in MHD, specifically examining laminar two-dimensional incompressible nanofluids flowing over an inclined porous surface under stretching conditions.

Shaw et al. [11] investigated the flow of magnetized graphene oxide and alumina nanoparticles through a narrow needle within a porous medium where the flow stops. Wakif et al. [12] employed the Buongiorno nanofluid model to study the impacts of thermal radiation and surface irregularities on thermo-magnetohydrodynamic. Heat exchange due to thermal radiation refers to the transfer of heat energy between surfaces or bodies via electromagnetic waves emitted because of their temperatures. Thermal radiation plays a key role in designing thermal comfort and material testing techniques. In astronomy, it helps study the temperature and composition of celestial objects. When it comes to heat transfer, thermal radiation can happen even in a vacuum, unlike conduction and convection, which need a medium.

The temperature and emissivity of the involved surfaces are two examples of parameters that influence the amount of heat exchanged through thermal radiation. It is also important to remember that thermal radiation might not be the optimal choice when designing thermal devices that experience significant temperature variations. Benos et al. [13] and Ibrahim et al. [14] performed a numerical analysis of unsteady fluid flow in two dimensions that included radiative effects. Their study revealed that temperature profiles rose as radiation factors and Ecker numbers increased. Rao and Deka [15] examined how thermal radiation and chemical reactivity influence the MHD flow of Casson nanofluid caused by a stretched sheet. Kumar et al. [16] studied the movement of Casson fluid along a stretching curved surface under thermal radiation effects, using Runge-Kutta and shooting methods for analysis.

Early in the 20th century, German physicist and engineer Ludwig Prandtl introduced the concept of boundary layer flow. The idea was first proposed in 1904 by Prandtl to explain how fluid flow behaves close to solid limits. Boundary layer flow over a permeable surface describes the phenomenon where a thin layer of fluid adjacent to a surface experiences distinct flow characteristics. When the surface is permeable, it allows fluid to pass through, influencing the flow within the boundary layer. Okechi et al. [17] investigated MHD flow through a sinusoidal boundary and observed that the effect of boundary waviness decreases under high magnetic field conditions, and found that the flow rate increases with lower wave numbers. Waini et al. [18] describe the flow and heat transfer properties of a hybrid nanofluid over a permeable sheet. Gowda et al. [19] explore effects of activation heat and chemical processes on energy transfer in a non-Newtonian nanofluid's Marangoni flow.

Based on the above-mentioned research work, no study has examined the flow of a hybrid nanoliquid over a movable surface, considering the inclined magnetic effect numerically.

This study investigates how a hybrid nanofluid behaves in an inclined magnetic field when thermal radiation is present. Similarity variables are employed to transform the partial differential equations into ordinary differential equations. The results are produced using the Keller box numerical method. We are confident that the novel theoretical conclusions made in this work are innovative.

2. Mathematical Formulation

This study examines the boundary layer flow of a hybrid nanofluid over a permeable flat plate. The coordinate system uses x along the plate and y perpendicular to it. The flow is possible for $y \geq 0$. In addition, the Uλ indicates the velocity of the plate, where λ corresponds to the moving plate, when $\lambda > 0$ it shows the flow moving away from the plate in the same direction, whereas it moves towards the origin when $\lambda < 0$ in the opposite direction as shown in Figure 1. Furthermore, v_w indicates the velocity for suction injection $v_w < 0$ while for injection it becomes $v_w > 0$. The magnetic field, as given by Aly et al. [20], is equal to $B = B_0 x^{-\frac{1}{2}}$.

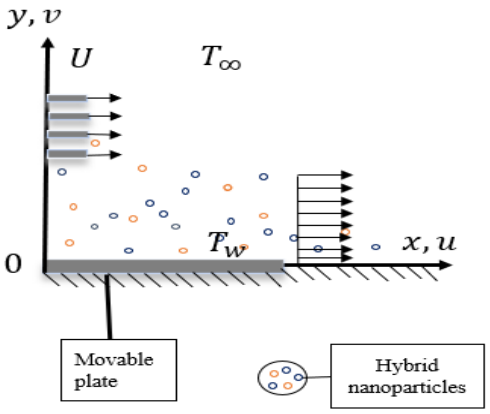

Figure 1. Physical representation using a coordinate system.

Based on these assumptions, it can be expressed as Devi and Devi [21]:

$$\frac{\partial u}{\partial x} + \frac{\partial v}{\partial y} = 0 \tag{1}$$

$$u\frac{\partial u}{\partial x} + v\frac{\partial u}{\partial y} = \frac{\mu_{hnf}}{\rho_{hn_f}}\frac{\partial^2 u}{\partial y^2} - \frac{\sigma_{hnf}}{\rho_{hnf}}B^2(u - U)sin^2\gamma \tag{2}$$

$$u\frac{\partial T}{\partial x}v\frac{\partial T}{\partial y} = \frac{k_{hnf}}{(\rho C_P)_{hnf}}\frac{\partial^2 T}{\partial y^2} - \frac{1}{(\rho C_P)_{hnf}}\frac{\partial q_r}{\partial y} + \frac{\sigma_{hnf}}{(\rho C_P)_{hnf}}B^2(u - \mathrm{U})^2\sin^2\gamma \tag{3}$$

The Rosseland approximation describes the radiation flux as, $q_r = \frac{-4\sigma^*}{3k^*}\frac{\partial T^4}{\partial y}$.

Here, k^* is considered the mean absorption coefficient and σ^* the Stefan-Boltzmann constant. This allows for expansion of T^4 in a Taylor series to be around T_∞, with higher-order terms being neglected $T^4 \cong 4T_\infty^3 T - 3T_\infty^4$, The linked boundary conditions are

$$u = \lambda U, \quad v = v_w, \ T = T_w \quad \text{at} \quad y = 0 \, , \ u \to U \, , \ T \to T_\infty \, , u \to U \, , \ T \to T_\infty \ as \ \ y \to \infty \tag{4}$$

Table 1. Given Takabi and Salehi [22], correlation hybrid nanofluids

Properties	**Hybrid nanofluid**
Density (ρ)	$\rho_{hnf} = (1-\phi_{hnf})\rho_f + \phi_1\rho_{s1} + \phi_2\rho_{s2}$
Heat Capacity (ρC_p)	$(\rho C_p)_{hnf} = (1-\phi_{hnf})(\rho C_p)_f + \phi_1(\rho C_p)_{s1} + \phi_2(\rho C_p)_{s2}$
Dynamic Viscosity (μ)	$\frac{\mu_{hnf}}{\mu_f} = \frac{1}{(1-\phi_{hnf})^{2.5}}$
Thermal conductivity (k)	$\frac{k_{hnf}}{k_f} = \left[\frac{\frac{\phi_1 k_1 + \phi_2 k_2}{\phi_{hnf}} + 2k_f + 2(\phi_1 k_1 + \phi_2 k_2) - 2\phi_{hnf} k_f}{\frac{\phi_1 k_1 + \phi_2 k_2}{\phi_{hnf}} + 2k_f - (\phi_1 k_1 + \phi_2 k_2) + \phi_{hnf} k_f}\right]$
Electrical conductivity (σ)	$\frac{\sigma_{hnf}}{\sigma_f} = \left[\frac{\frac{\phi_1 \sigma_1 + \phi_2 \sigma_2}{\phi_{hnf}} + 2\sigma_f + 2(\phi_1 \sigma_1 + \phi_2 \sigma_2) - 2\phi_{hnf} \sigma_f}{\frac{\phi_1 \sigma_1 + \phi_2 \sigma_2}{\phi_{hnf}} + 2\sigma_f - (\phi_1 \sigma_1 + \phi_2 \sigma_2) + \phi_{hnf} \sigma_f}\right]$

Table 2. Oztop and Abu-Nada [23] thermophysical characteristics for pure water and nanoparticles

Thermophysical Property	Unit	Pure Water	Al_2O_3	CuO
Density (ρ)	kg/m^3	997.1	3970	8933
Specific Heat (Cp)	J/(kg·K)	4179	765	385
Thermal Conductivity (k)	W/(m·K)	0.613	40	400

Hence, the similarity variables are:

$$u = Uf'(\eta), v = \sqrt{\frac{Uv_f}{2x}}[\eta f'(\eta) - f(\eta)], \eta = y\sqrt{\frac{U}{2xv_f}},$$

$$\psi = \sqrt{2v_f x U} f(\eta) \, , \ \theta(\eta) = \frac{T - T\infty}{T_w - T_\infty}. \tag{5}$$

While the transpiration effect is defined as

$$v_w = -\sqrt{\frac{Uv_f}{2x}} S. \tag{6}$$

Here, suction and injection are indicated by S > 0 and S < 0, where S denotes the mass flux velocity. These are the converted ODEs and boundary conditions obtained by substituting (6) into Equations (2) and (3).

$$ff'' + \frac{\frac{\mu_{hnf}}{\mu_f}}{\frac{\rho_{hnf}}{\rho_f}} f''' - \frac{\frac{\sigma_{hnf}}{\sigma_f}}{\frac{\rho_{hnf}}{\rho_f}} M(f'-1)\sin^2\gamma = 0 \tag{7}$$

$$f\theta' + \frac{\frac{\sigma_{hnf}}{\sigma_f}}{\frac{(\rho C_P)_{hnf}}{(\rho C_P)_f}} EcM(f'-1)^2\sin^2\gamma + \frac{1}{Pr}\left(\frac{1}{\rho C_p}\right)_{hnf}(k_{hnf} + \frac{4}{3}\alpha N)\theta'' = 0 \tag{8}$$

$$f'(0) = \lambda, f(0) = S, \theta(0) = 1, \text{ at } \eta = 0,$$

$$f'(\eta) \to 1, \theta(\eta) \to 0 \quad \text{as} \quad \eta \to \infty. \tag{9}$$

The symbols for the radiation parameter N, the magnetic parameter is M, the Eckert number is Ec, and the Prandtl number is Pr. The physical quantities of significance are the skin friction coefficient C_f and the local Nusselt number Nu_x. These parameters are defined as

$$Pr = \frac{(\mu C_P)_f}{k_f}, \; M = \frac{2\sigma_f B_0^2}{U\rho_f}, \; Ec = \frac{U^2}{(C_p)_f(T_w - T_\infty)} \tag{10}$$

$$C_f = \frac{\mu_{hnf}}{\rho_f U^2}\left(\frac{\partial u}{\partial y}\right)_{y=0}, Nu_x = -\frac{xk_{hnf}}{k_f(T_w - T_\infty)}\left(\frac{\partial T}{\partial y}\right)_{y=0}, \; N = \frac{4\sigma^* T_\infty^3}{k^*\alpha} \tag{11}$$

Through applying, we can get the parameters such that

$$\sqrt{2}Re_x^{1/2}C_f = \frac{\mu_{hnf}}{\mu_f}f''(0), \sqrt{2}Re_x^{-1/2}Nu_x = -\frac{k_{hnf}}{k_f}\theta'(0) \tag{12}$$

And the local Reynolds number is $Re_x = \frac{Ux}{v_f}$

3. Results and Discussion

The main features of flow and heat transfer in a magnetohydrodynamics boundary layer over a permeable sheet are analyzed using hybrid nanofluids in the working fluids. To thoroughly understand the physical problem, numerous numerical solutions are obtained for different values of the physical parameters. The nonlinear ordinary differential equation (7) and Equation (8) are solved numerically in MATLAB employing the Keller box method for specific parameter values. Additionally, the boundary conditions in Equation (9) are addressed with numerical methods. The temperature profile $\theta(\eta)$, the velocity profile $f'(\eta)$, against the magnetic parameter M, the radiation parameter N, the suction/injection parameter S, with fixed Prandtl number Pr at $Pr = 6.2$ (water) are the graphs obtained numerically.

The Keller box method, or finite volume method (FVM) is a numerical technique utilized to solve ODE's especially in fluid dynamics and heat transfer phenomena. It discretizes the domain into a grid (or boxes) and integrates the PDEs over these finite volumes. Two solutions are predicted to exist for various involved parameter values. The freestream flow and moving plate are travelling in the same direction when $\lambda > 0$. Conversely, when $\lambda < 0$ they move in opposite directions. Other parameters based on the solution domain are defined as

$0 \leq S \leq 0.5$, $0 \leq M \leq 0.02$, $0 \leq Ec \leq 1$, $0 \leq \varphi_1, \varphi_2 \leq 0.01$.

Where φ_1 and φ_2 are nanoparticle volume fractions. When there are dual solutions, it is feasible for there to be two different values of η_∞, which would lead to two separate velocity profiles $f'(\eta)$ and temperature profiles $\theta(\eta)$. Table 3 and Table 4 display the results of a few validation tests that were undertaken before generating the solutions. These tests confirm the accuracy of the current model.

Since the primary focus of this work is on hybrid fluid and magnetic field, comparisons are restricted to viscous working fluids and single fluids without the control parameter. The different values of S in regular fluid are compiled by Weidman et al. [24] when $\varphi_1 = \varphi_2 = 0$ and $M = 0$ (presented in Table 3). Meanwhile, Table 4, which is consistent with Rohni et al. [25], shows the available solutions of $\varphi_1 = 0$, $\varphi_2 = 0.1$ and $M = S = R = 0$.

Table 3. Validation test using suction/injection parameter for the critical value λ_c.

S	Weidman et al. [24]	Khashi'ie et al. [26]	Present
-0.50	-0.1035	-0.10388	-0.10389
-0.25	-0.2125	-0.21461	-0.21463
0.00	-0.3541	-0.35410	-0.35411
0.25	-0.5224	-0.52238	-0.52239
0.50	-0.7200	-0.72001	-0.72002

Table 4. First and second solutions of $f''(0)$ when $M = S = R = 0$ and $\varphi_1 = 0$, φ_2 =0.1

$\boldsymbol{\lambda}$	Rohni et al. [25]		Khashi'ie et al. [26]		Present	
	First	Second	First	Second	First	Second
-0.1000	0.5416	0.0023	0.541615	0.002274	0.541614	0.002285
-0.1500	0.5276	0.0102	0.527547	0.010169	0.527657	0.010170
-0.2000	0.5053	0.0261	0.505318	0.026061	0.505329	0.026172
-0.2500	0.4717	0.0533	0.471688	0.053322	0.471789	0.053333
-0.3000	0.4190	0.0997	0.418959	0.099702	0.419060	0.099713
-0.3500	0.3028	0.2098	0.302592	0.209761	0.302801	0.209872
-0.3541	0.2623	--	0.257961	0.253877	0.262380	--

Figures 2 and 3 show velocity profiles $f'(\eta)$ for various values of solid volume fractions φ_1 and φ_2 with the influence of $M = 0.1$,0.5 when, $N = 0.1$, $Pr = 6.5$, $Ec = 0.1$, $\lambda = 1.0$, $S = 1.0$, $\varphi_1 = 0.1$ and $\varphi_2 = 0.1$ and $\gamma = 45^o$ as given in Figure 2. Note that the magnetic field affects the velocity profile when $\lambda > 1$. The difference between first and second solutions is the fluid

velocity decrements. Essentially, the magnetic field resists fluid movement through a drag called the Lorentz force, which slows down boundary layer separation.

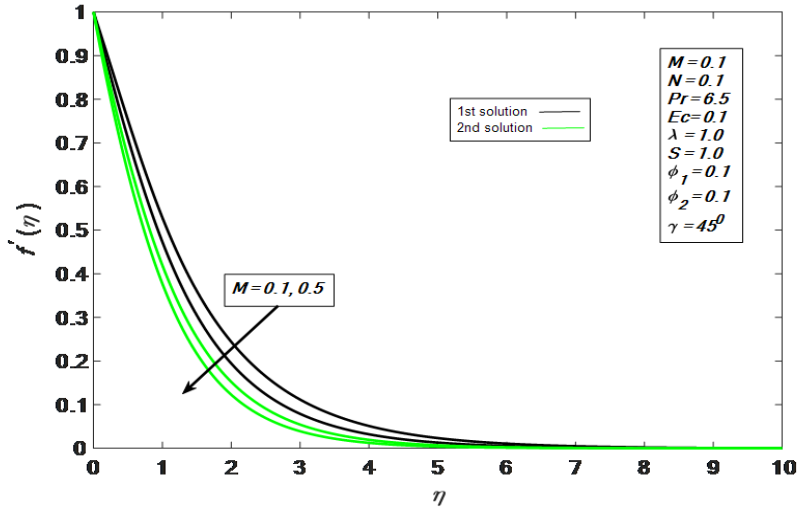

Figure 2. Velocity profile $f'(\eta)$ variation for various M values

The velocity $f'(\eta)$ profile is shown in Figure 3, together with the influence of $M = 0.1,0.2$ versus a wide range of parameters, such as $M = 0.1$, $Pr = 6.5$, $Ec = 0.1$, $\lambda = -1.2$, $S = 1.0$, $\varphi_1 = 0.1$, $\varphi_2 = 0.1$, and the inclination angle $\gamma = 45^o$. Regarding the impact of the magnetic field on the velocity profile, this concerns the difference in fluid velocity increments between the first and second solutions. Temperature can be increased by physically dispersing more energy, which is achieved by raising the volume fraction of nanoparticles.

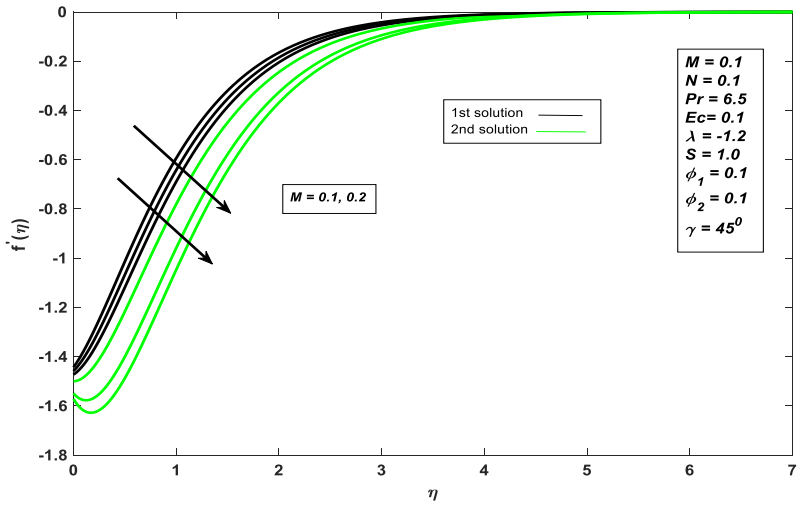

Figure 3. Velocity profile $f'(\eta)$ variation for various M values

The suction parameter influences dimensionless velocity $f'(\eta)$ profiles shown in Figure 4. These profiles include the effects of suction parameter S = 0.1,0.2, along with several

additional factors, such as $M = 0.1$, $N = 0.1$, $Pr = 6.5$, $Ec = 0.1$, $\lambda = 1.0$, $\gamma = 45^o$, $\varphi_1 = 0.1$ and $\varphi_2 = 0.1$. An increase in the suction parameter tends to draw fluid into a void, thereby altering the boundary layer. As a result, increasing the suction parameter causes the velocity to decrease in both solutions.

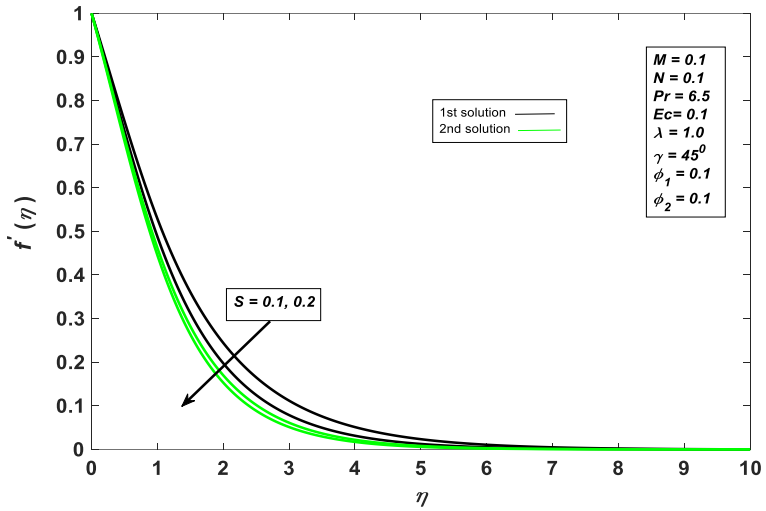

Figure 4. Velocity profile $f'(\eta)$ variation for various S values

The impact of an aligned angle γ on velocity profiles is seen in Figure 5. Based on different values of the parameter $\gamma = 1^o, 30^o$ and shows the $f'(\eta)$ profile for a range of parameters, such as $N = 0.1$, $Pr = 6.5$, $Ec = 0.1$, $\lambda = 1.0$, $S = 0.1$, $\varphi_1 = 0.1$ and $\varphi_2 = 0.1$ The velocity profile falls as the angle of inclination rises. As γ grows, the boundary layer's thickness correspondingly decreases.

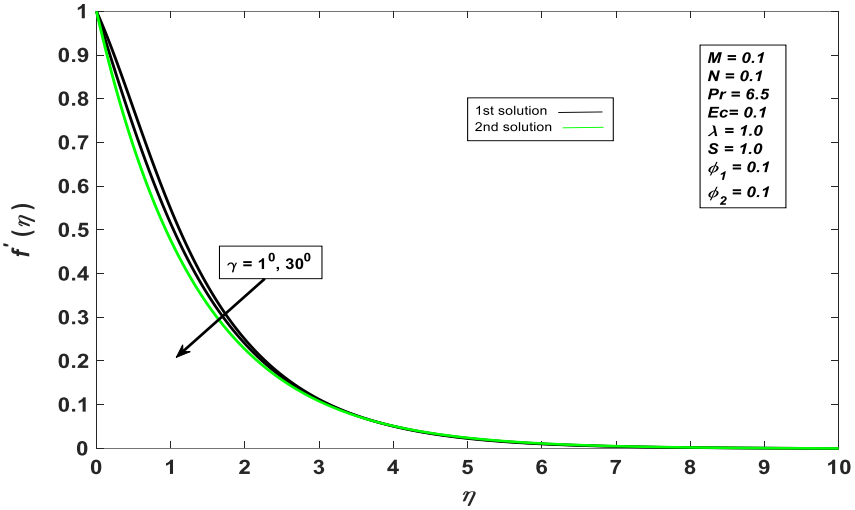

Figure 5. Velocity profile $f'(\eta)$ variation for various γ values

The temperature profile, represented as $\theta(\eta)$ in Figure 6, illustrates the impact of the Eckert numbers $Ec = 0.1$ and 0.3 on several parameters, including $M = 0.1$, $N = 0.1$, Pr =0.1,

$S = 0.5$, $\lambda = 1.2$ $\gamma = 45^o$, $\varphi_1 = 0.1$ and $\varphi_2 = 0.1$. As the temperature profile increases, the boundary layer viscosity also increases, while the Eckert number decreases. Even with a higher Eckert number, the kinetic energy of the fluid flow exceeds the thermal energy involved. This greater kinetic energy enhances heat transfer and fluid mixing, leading to more efficient thermal energy distribution throughout the system and an overall rise in temperature.

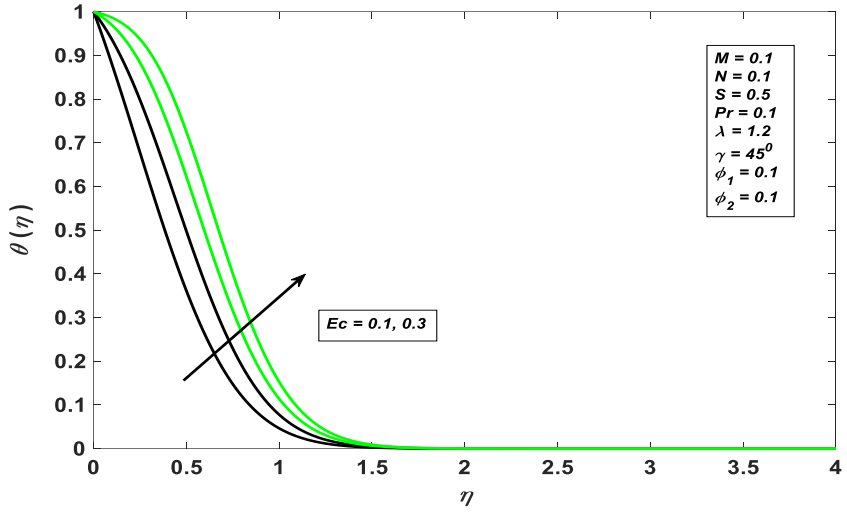

Figure 6. Temperature profile $\theta(\eta)$ variation for various Ec values

Figure 7 illustrates the relationship between the temperature profile and the radiation parameter N, showing the temperature plotted $\theta(\eta)$ profile alongside the effects of the radiation parameter $N = 0,1$ and 2. The analysis includes other parameters such as $M = 0.1$, $Pr = 2.0$, $S = 0.5$, $Ec = 0.1$, $\lambda = 1.0$, $\gamma = 45^o$, $\varphi_1 = 0.1$ and $\varphi_2 = 0.1$. As the radiation parameter decreases, the temperature profile also increases. As a result, heat is produced by the flow field, raising the thermal layer's temperature.

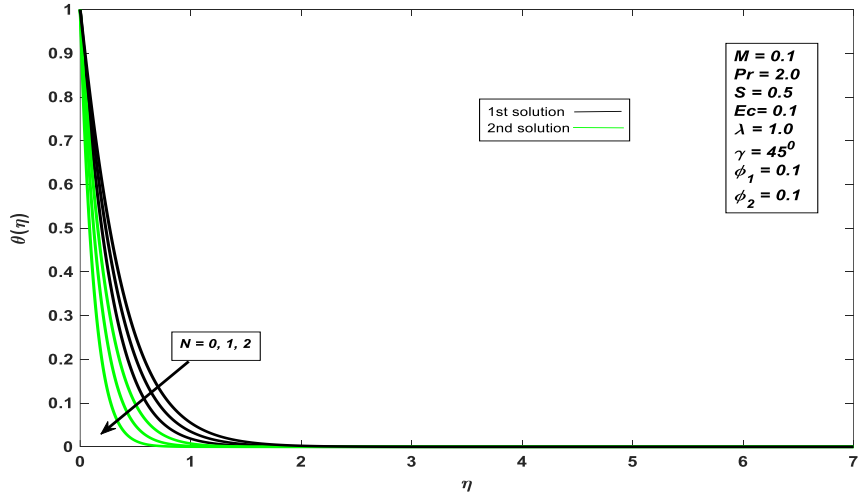

Figure 7. Temperature profile $\theta(\eta)$ variation for various N values

4. Conclusion

In this study, we investigate the MHD boundary layer flow of hybrid nanofluid flow over a permeable moving surface. In addition, an inclined magnetic field along with radiation effects is taken into consideration. Moreover, it is analysed how Joule heating effects affect the flow phenomenon of the hybrid nanoliquid. The Keller box method in MATLAB is utilized to solve the system of ordinary differential equations created by applying a similarity transformation to the governing partial differential equations. Standard boundary layer flow approximations are then applied to the physical phenomena. Tables and graphs are representing the calculated findings. Two solutions are seen when $\lambda_c < \lambda \leq 0$.

The effects of various parameters are studied in this research. This study examines various parameters, including velocity, temperature, and skin friction. The velocity profile decreases for different values of M, suction S and in γ. The temperature profile increases for values of Eckert (Ec) and decreases for the radiation parameter N. The findings of this study suggest that the heating and cooling sectors improve heat transfer efficiency by introducing a small-scale magnetic field and suction.

Acknowledgement: The authors extend their appreciation to the Arab Open University for funding this work through the AOU research fund No. (AOURG-2025-048).

Conflicts of Interest: The authors declare that there are no conflicts of interest regarding the publication of this paper.

References

[1] S.U.S. Choi, D.A. Singer, H.P. Wang, Developments and Applications of Non-Newtonian Flows, in: 1995 ASME International Mechanical Engineering Congress and Exposition, San Francisco, California, 1995.

[2] J. Prakash, D. Tripathi, A.K. Tiwari, S.M. Sait, R. Ellahi, Peristaltic Pumping of Nanofluids Through a Tapered Channel in a Porous Environment: Applications in Blood Flow, Symmetry 11 (2019), 868. https://doi.org/10.3390/sym11070868.

[3] G. Huminic, A. Huminic, Entropy Generation of Nanofluid and Hybrid Nanofluid Flow in Thermal Systems: A Review, J. Mol. Liq. 302 (2020), 112533. https://doi.org/10.1016/j.molliq.2020.112533.

[4] M. Molana, R. Ghasemiasl, T. Armaghani, A Different Look at the Effect of Temperature on the Nanofluids Thermal Conductivity: Focus on the Experimental-Based Models, J. Therm. Anal. Calorim. 147 (2021), 4553-4577. https://doi.org/10.1007/s10973-021-10836-w.

[5] E.H. Aly, I. Pop, Mhd Flow and Heat Transfer Near Stagnation Point Over a Stretching/shrinking Surface with Partial Slip and Viscous Dissipation: Hybrid Nanofluid Versus Nanofluid, Powder Technol. 367 (2020), 192-205. https://doi.org/10.1016/j.powtec.2020.03.030.

[6] N.A.L. Aladdin, N. Bachok, I. Pop, Cu-al2o3/water Hybrid Nanofluid Flow Over a Permeable Moving Surface in Presence of Hydromagnetic and Suction Effects, Alex. Eng. J. 59 (2020), 657-666. https://doi.org/10.1016/j.aej.2020.01.028.

[7] N.A. Zainal, R. Nazar, K. Naganthran, I. Pop, Mhd Flow and Heat Transfer of Hybrid Nanofluid Over a Permeable Moving Surface in the Presence of Thermal Radiation, Int. J. Numer. Methods Heat Fluid Flow 31 (2020), 858-879. https://doi.org/10.1108/hff-03-2020-0126.

[8] B.S. Goud, J.V. Madhu, M.R. Shekar, Mhd Viscous Dissipative Fluid Flows in a Channel with a Stretching and Porous Plate with Radiation Effect, Int. J. Innov. Technol. Explor. Eng. 8 (2019), 1877-1882. https://doi.org/10.35940/ijitee.k2086.0981119.

[9] A.J. Chamkha, A.S. Dogonchi, D.D. Ganji, Magneto-hydrodynamic Flow and Heat Transfer of a Hybrid Nanofluid in a Rotating System Among Two Surfaces in the Presence of Thermal Radiation and Joule Heating, AIP Adv. 9 (2019), 025103. https://doi.org/10.1063/1.5086247.

[10] S. Reza-E-Rabbi, M.S. Khan, S. Arifuzzaman, S. Islam, P. Biswas, B. Rana, A. Al-Mamun, T. Hayat, S.F. Ahmmed, Numerical Simulation of a Non-Linear Nanofluidic Model to Characterise the Mhd Chemically Reactive Flow Past an Inclined Stretching Surface, Partial. Differ. Equ. Appl. Math. 5 (2022), 100332. https://doi.org/10.1016/j.padiff.2022.100332.

[11] S. Shaw, F. Mabood, T. Muhammad, M.K. Nayak, M. Alghamdi, Numerical Simulation for Entropy Optimized Nonlinear Radiative Flow of GO-Al_2O_3 Magneto Nanomaterials with Autocatalysis Chemical Reaction, Numer. Methods Partial. Differ. Equ. 38 (2022), 329–358. https://doi.org/10.1002/num.22623.

[12] A. Wakif, A. Chamkha, T. Thumma, I.L. Animasaun, R. Sehaqui, Thermal Radiation and Surface Roughness Effects on the Thermo-Magneto-Hydrodynamic Stability of Alumina–Copper Oxide Hybrid Nanofluids Utilizing the Generalized Buongiorno's Nanofluid Model, J. Therm. Anal. Calorim. 143 (2020), 1201-1220. https://doi.org/10.1007/s10973-020-09488-z.

[13] L. Benos, U. Mahabaleshwar, P. Sakanaka, I. Sarris, Thermal Analysis of the Unsteady Sheet Stretching Subject to Slip and Magnetohydrodynamic Effects, Therm. Sci. Eng. Prog. 13 (2019), 100367. https://doi.org/10.1016/j.tsep.2019.100367.

[14] M. Ibrahim, T. Saeed, S. Zeb, Numerical Simulation of Time-Dependent Two-Dimensional Viscous Fluid Flow with Thermal Radiation, Eur. Phys. J. Plus 137 (2022), 609. https://doi.org/10.1140/epjp/s13360-022-02813-5.

[15] S. Rao, P. Deka, A Numerical Solution Using Efdm for Unsteady Mhd Radiative Casson Nanofluid Flow Over a Porous Stretching Sheet with Stability Analysis, Heat Transf. 51 (2022), 8020-8042. https://doi.org/10.1002/htj.22679.

[16] K. Anantha Kumar, V. Sugunamma, N. Sandeep, Effect of Thermal Radiation on Mhd Casson Fluid Flow Over an Exponentially Stretching Curved Sheet, J. Therm. Anal. Calorim. 140 (2019), 2377-2385. https://doi.org/10.1007/s10973-019-08977-0.

[17] N.F. Okechi, S. Asghar, D. Charreh, Magnetohydrodynamic Flow Through a Wavy Curved Channel, AIP Adv. 10 (2020), 035114. https://doi.org/10.1063/1.5142214.

[18] I. Waini, A. Ishak, I. Pop, Hybrid Nanofluid Flow and Heat Transfer Over a Permeable Biaxial Stretching/shrinking Sheet, Int. J. Numer. Methods Heat Fluid Flow 30 (2019), 3497-3513. https://doi.org/10.1108/hff-07-2019-0557.

[19] R.J. Punith Gowda, R. Naveen Kumar, A.M. Jyothi, B.C. Prasannakumara, I.E. Sarris, Impact of Binary Chemical Reaction and Activation Energy on Heat and Mass Transfer of Marangoni Driven Boundary Layer Flow of a Non-Newtonian Nanofluid, Processes 9 (2021), 702. https://doi.org/10.3390/pr9040702.

[20] E.H. Aly, M. Benlahsen, M. Guedda, Similarity Solutions of a Mhd Boundary-Layer Flow Past a Continuous Moving Surface, Int. J. Eng. Sci. 45 (2007), 486-503. https://doi.org/10.1016/j.ijengsci.2007.04.016.

[21] S.P.A. Devi, S.S.U. Devi, Numerical Investigation of Hydromagnetic Hybrid Cu–Al_2O_3/Water Nanofluid Flow Over a Permeable Stretching Sheet with Suction, Int. J. Nonlinear Sci. Numer. Simul. 17 (2016), 249-257. https://doi.org/10.1515/ijnsns-2016-0037.

[22] B. Takabi, S. Salehi, Augmentation of the Heat Transfer Performance of a Sinusoidal Corrugated Enclosure by Employing Hybrid Nanofluid, Adv. Mech. Eng. 6 (2014), 147059. https://doi.org/10.1155/2014/147059.

[23] H.F. Oztop, E. Abu-Nada, Numerical Study of Natural Convection in Partially Heated Rectangular Enclosures Filled with Nanofluids, Int. J. Heat Fluid Flow 29 (2008), 1326-1336. https://doi.org/10.1016/j.ijheatfluidflow.2008.04.009.

[24] P. Weidman, D. Kubitschek, A. Davis, The Effect of Transpiration on Self-Similar Boundary Layer Flow Over Moving Surfaces, Int. J. Eng. Sci. 44 (2006), 730-737. https://doi.org/10.1016/j.ijengsci.2006.04.005.

[25] A. Mohd Rohni, S. Ahmad, I. Pop, Boundary Layer Flow Over a Moving Surface in a Nanofluid Beneath a Uniform Free Stream, Int. J. Numer. Methods Heat Fluid Flow 21 (2011), 828-846. https://doi.org/10.1108/09615531111162819.

[26] N.S. Khashi'ie, N.M. Arifin, I. Pop, Magnetohydrodynamics (mhd) Boundary Layer Flow of Hybrid Nanofluid Over a Moving Plate with Joule Heating, Alex. Eng. J. 61 (2022), 1938-1945. https://doi.org/10.1016/j.aej.2021.07.032.